Neurite Outgrowth from Bipolar and Horizontal Cells after Experimental Retinal Detachment

Geoffrey P. Lewis,[1] *Kenneth A. Linberg,*[1] *and Steven K. Fisher*[1,2]

Purpose. To study the responses of horizontal cells and rod bipolar cells, the second-order neurons in the retina, to the degeneration induced by experimental retinal detachment.

Methods. Retinas from the eyes of domestic cats were examined 1, 3, 7, and 28 days after detachment using immunocytochemical and electron microscopic analyses. Retinal sections were labeled with antibodies to synaptophysin, calbindin D, and protein kinase C (PKC), proteins that serve as markers for synaptic terminals, horizontal cells, and rod bipolar cells, respectively.

Results. Beginning 1 day after detachment, the outer plexiform layer becomes disorganized and synaptophysin-labeled photoreceptor terminals are detected among the cell bodies of photoreceptors in the outer nuclear layer (ONL). At the same time, horizontal and rod bipolar cell processes grow into the ONL. In some cases, these processes contact photoreceptor terminals that have withdrawn deep into the ONL. Double-labeling experiments with antibodies to glial fibrillary acidic protein (Müller cell labeling) and phosphodiesterase γ (cone labeling) demonstrate that the calbindin D- and PKC-positive neurite outgrowths are not derived from either Müller cells or cone photoreceptors.

Conclusions. Horizontal and rod bipolar cell processes lengthen after retinal detachment, perhaps in response to a withdrawal of their presynaptic targets, the photoreceptor synaptic terminals. This apparent attempt to maintain synaptic contact after injury demonstrates a plasticity in the adult retina that may be of importance for the recovery of vision in human patients. (*Invest Ophthalmol Vis Sci.* 1998;39:424-434)

In the normal retina, the light-sensitive outer segments of the photoreceptor cells are interdigitated with the highly specialized apical processes of the retinal pigment epithelial cells. Numerous cellular and molecular interactions occur across this interface, including the transport of oxygen, various ions, and vitamin A and the phagocytosis by the retinal pigment epithelium of aged outer segment membranes shed by the photoreceptor cells.[1] The physical separation of these two layers (retinal detachment) is a serious cause of visual impairment in humans and can result from many different causes, including penetrating wounds to the eye and retinal tears and from the complications of diabetes, age-related macular degeneration, and proliferative diseases of the eye. Animal models of this condition have demonstrated a rapid degeneration of photoreceptor outer segments in detached retinas[2] and the loss of varying numbers of photoreceptor cells by apoptotic and perhaps necrotic cell death.[3,4] The loss of photoreceptors and the imperfect regeneration of outer segments after retinal reattachment have generally been assumed to underlie the visual deficits that can result even after anatomically successful reattachment surgery.

In this study, we used various antibodies in conjunction with immunofluorescence imaging by confocal microscopic analysis to study the responses of photoreceptor synaptic terminals, horizontal cells, and rod bipolar cells to retinal detachment. We found that, as photoreceptor synaptic terminals retract from the outer plexiform layer (OPL), the interneurons extend their processes to the outer nuclear layer (ONL). These events are detectable within 1 day of detachment. This plasticity in second-order neurons may affect the ability of the retina to recover from detachment and perhaps from other photoreceptor degenerative diseases as well.

Methods

Retinal Detachments

Retinal detachments were produced in the right eyes of adult cats (>6 months of age) as described previously.[5] Briefly, the lens was removed, and the eye was allowed to heal for 2 weeks. After removal of the vitreous, a solution of 0.25% sodium hyaluronate (Healon; Pharmacia, Piscataway, NJ) was infused between the neural retina and the retinal pigment epithelium by means of a micropipette. Three animals each were killed at 1, 3, 7, and 28 days after detachment. Cats were initially entrained to a 12-hour light-12-hour dark cycle and were killed 4 hours after light onset, at which time the retinas were processed for immunocytochemical and electron microscopic analyses. All procedures adhered to the tenets of the ARVO Statement for the Use of Animals in Ophthalmic and Vision Research.

From the [1]Neuroscience Research Institute and [2]Molecular, Cellular, and Developmental Biology, University of California, Santa Barbara, California.

Supported by United States Public Health Service Research grant EY-00888.

Submitted for publication November 11, 1997; revised October 23, 1997; accepted November 3, 1997.

Proprietary interest category: N.

Reprint requests: Geoffrey P. Lewis, Neuroscience Research Institute, University of California, Santa Barbara, CA 93106-5060.

Investigative Ophthalmology & Visual Science, February 1998, Vol. 39, No. 2

Immunocytochemical Analysis

Retinal samples were prepared for confocal microscopy as described previously.[6] Briefly, retinas were cut into quadrants and fixed in 4% paraformaldehyde in sodium cacodylate buffer (0.1 N; pH 7.4) for 2 hours. Tissue samples, approximately 2-mm square, were excised and embedded in 5% agarose in phosphate-buffered saline (PBS). Sections of 100-μm thickness were cut on a vibratome (Technical Products International, Polysciences, Warrington, PA) and incubated in normal donkey serum (1:20) overnight at 4°C on a rotator. On the following day, the blocking serum was removed and the sections were incubated overnight in primary antibodies at 4°C. All antibodies were diluted in PBS containing 0.5% bovine serum albumin, 0.1% Triton X-100, and 0.1% sodium azide. The monoclonal antibody to protein kinase C (PKC) (clone MC5; Amersham, Arlington Heights, IL) was used at 1:50 dilution; the monoclonal antibody to calbindin D (Sigma Chemical, St. Louis, MO) was used at 1:1000; and the polyclonal antibody to synaptophysin (DAKO; Carpinteria, CA) was used at 1:50. The sections were rinsed in PBS containing bovine serum albumin (0.5%) and incubated in donkey anti-mouse immunogloblin G conjugated to the fluorochrome Cy3 (1:200; Jackson ImmunoResearch Laboratories, West Grove, PA) overnight at 4°C on a rotator. The sections were rinsed, mounted in 5% *n*-propyl gallate in glycerol, and viewed with a laser-scanning, confocal microscope (Bio-Rad 1024, Hercules, CA). In some cases, multiple planes of focus were collected (that is, a z-series) and then projected as a two-dimensional image. Each image plane represented 1 μm. The number of images projected is included in the figure captions.

Anti-calbindin D and anti-PKC were also used on retinal sections in a series of double-label experiments. The procedure is the same as described above, except that, after the blocking serum, the retinal sections were first incubated overnight in either antisynaptophysin, anti-glial fibrillary acidic protein (GFAP, 1:400; DAKO), or anti-phosphodiesterase γ (PDEγ, 1:1000; a gift from B. Fung, University of California at Los Angeles). These polyclonal antibodies were visualized using the secondary antibody, goat anti-rabbit immunogloblin G, conjugated to the fluorochrome fluorescein (Cappel, Durham, NC). After rinsing, the sections were fixed in 4% paraformaldehyde for 4 hours, rinsed, incubated overnight in the monoclonal antibodies to calbindin-D or PKC, and processed as described above.

Electron Microscopic Analysis

As described previously,[7] tissue was immersion fixed in 1% paraformaldehyde and 1% glutaraldehyde in sodium phosphate buffer (0.086 M; pH 7.3) for 24 hours, rinsed in buffer, fixed in phosphate-buffered osmium tetroxide (2%) for 1 hour, dehydrated in a graded ethanol series, and embedded in Spurr's resin. Thin (80-90 nm) sections were stained with uranyl acetate and lead citrate and viewed with an electron microscope (CM-10; Philips Electronic Instruments, Mahwah, NJ).

Electron Microscopic–Immunocytochemical Analysis

As described previously,[8] tissue was immersed in 1% paraformaldehyde and 1% glutaraldehyde in sodium phosphate buffer for 1 hour, dehydrated in a graded methanol series, and embedded in London Resin White (Polysciences). Uranyl acetate was added to 70% methanol during the dehydration to enhance contrast and to improve tissue preservation and the immunolabeling of proteins.

Thin sections (80-90 nm) were placed on nickel grids, incubated on drops of normal goat serum (1:50) for 30 minutes, blotted, and incubated overnight on drops containing anti-synaptophysin antibody (1:100). The next day the grids were rinsed in PBS-bovine serum albumin and incubated in goat anti-rabbit immunogloblin G conjugated to 15-nm gold spheres for 1 hour. The grids were rinsed in PBS- bovine serum albumin and distilled water, stained with uranyl acetate and lead citrate, and exposed to osmium tetroxide vapors (2% osmium in PBS) for 1 hour.

Results

Immunocytochemistry–Bipolar Cell Response

Immunocytochemical labeling on sections of normal retina with anti-PKC occurs exclusively in the rod bipolar cells (Fig. 1A). Fine rod bipolar cell dendrites in the OPL extend into the layer of rod synaptic terminals, and more robust labeling is present in the rod bipolar cell bodies, axons, and axon terminals. One day after retinal detachment, fine, sometimes beaded, PKC-positive processes extend into the ONL past the layer of rod terminals (Figs. 1B, 1C). In addition, Müller cells and astrocytes in the inner retina are faintly PKC positive (Fig. 1B). At 3 days after detachment, some processes of the rod bipolar cells extend through the ONL to the layer of photoreceptor inner segments (data not shown). This general pattern of labeling continues in the 28-day detachments, but an increase in the length and thickness of processes of the rod bipolar cells extends to the ONL (Fig. 1D). The anti-PKC labeling of Müller cells is always less intense than that of the rod bipolar cells and never extends into the outer retina (Fig. 1D). The pattern and intensity of labeling in the rod bipolar cell bodies, axons, and axon terminals is unchanged at all times after detachment.

To determine whether the extension of labeled neurites from the rod bipolar cells is related to changes in photoreceptor synaptic terminals after detachment, double-labeling experiments were performed using anti-synaptophysin and anti-PKC. Anti-synaptophysin labeling in the normal retina is present in the synaptic terminals of the rods and cones in the OPL (Fig. 2A). At 1 day after detachment, the layer of photoreceptor synaptic terminals becomes discontinuous and is interrupted by areas with little labeling. In such areas, many of the synaptophysin-positive terminals lie in the ONL (Fig. 2B; and see Electron Microscopic Analysis below). In these disrupted regions of the OPL, the newly formed, PKC-positive, rod bipolar cell dendrites extend into the ONL where they contact the synaptophysin-positive photoreceptor terminals (Fig. 2B; arrowheads).

To determine whether the anti-PKC-labeled processes in the ONL result from upregulated expression of PKC in Müller cells, double-labeling experiments were performed with anti-GFAP to mark the Müller cell processes in sections labeled with anti-PKC. Significant anti-PKC labeling occurs adjacent to the anti-GFAP labeling within the ONL, but the two signals do not overlap (Fig. 2C). This indicates that the PKC-positive processes are distinct from the anti-GFAP-labeled Müller cells.

Immunocytochemistry–Horizontal Cell Response

Immunolabeling with anti-calbindin D in normal retina is found in cone cell bodies and synaptic terminals, horizontal cells, and

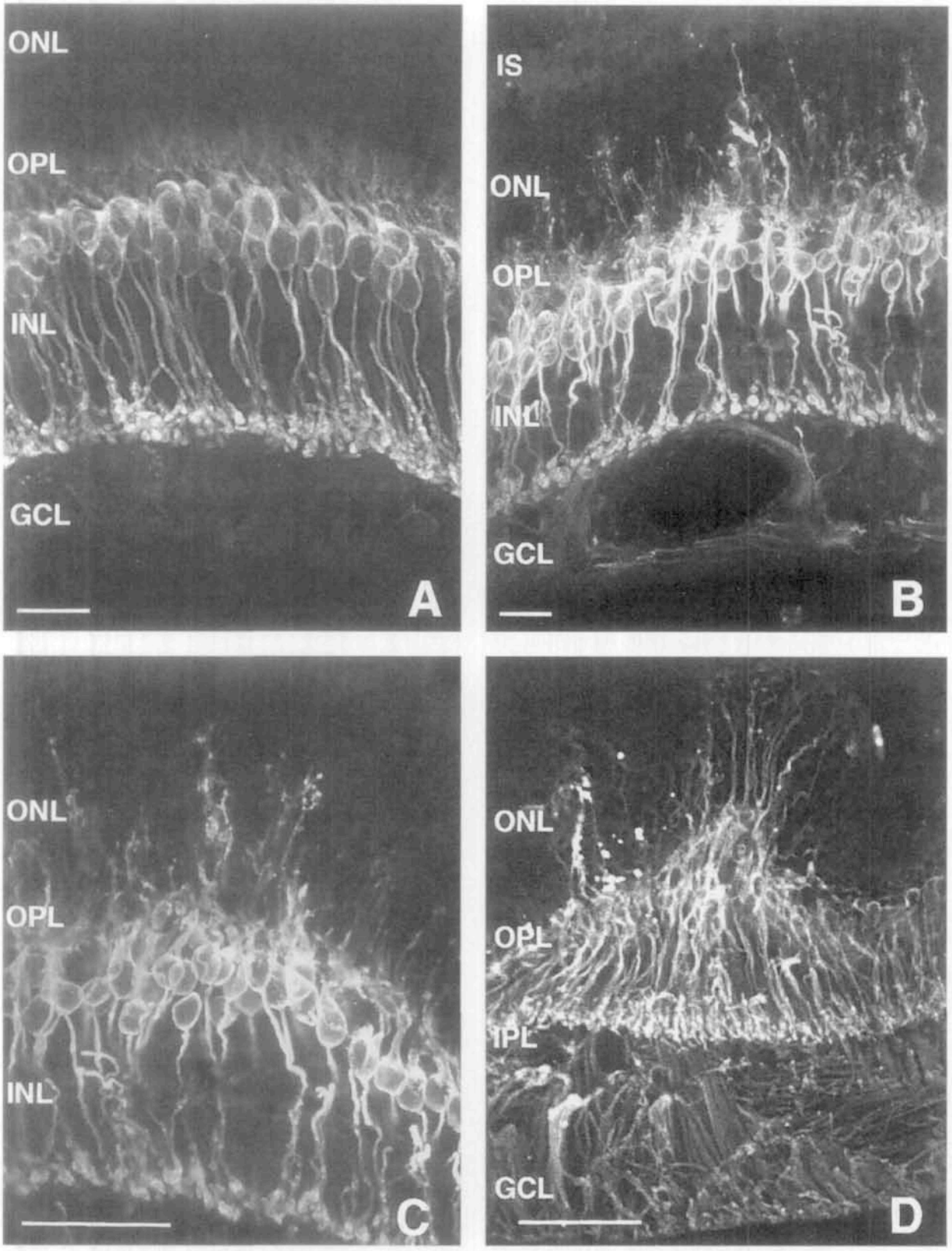

FIGURE 1. Anti-protein kinase C labeling of normal (**A**) and detached (**B**, **C**, **D**) retinal sections. (**A**) Normal retina. Labeling occurs only in the rod bipolar cells, including the fine dendritic processes in the outer plexiform layer (*OPL*), the cell bodies in the inner nuclear layer (*INL*), the axon, and the axon terminal. (**B**) 1-day retinal detachment. Labeling is present in bipolar cell processes extending into the outer nuclear layer (*ONL*). Faint labeling also begins to appear in other cell types in the ganglion cell layer (*GCL*). (**C**) 1-day retinal detachment. Higher magnification of the bipolar cell labeling in the ONL in a different area than shown in **C**. (**D**) 28-day retinal detachment. Low magnification showing labeled bipolar cell processes extending into the ONL. The fainter signal in the inner retina is from other cell types, including Müller cell and astrocyte processes, and does not extend past the inner plexiform layer (*IPL*). **A**, **C**, and **D** are projections of nine images; **B**, is a projection of 13 images. *Bars*, 20 μm.

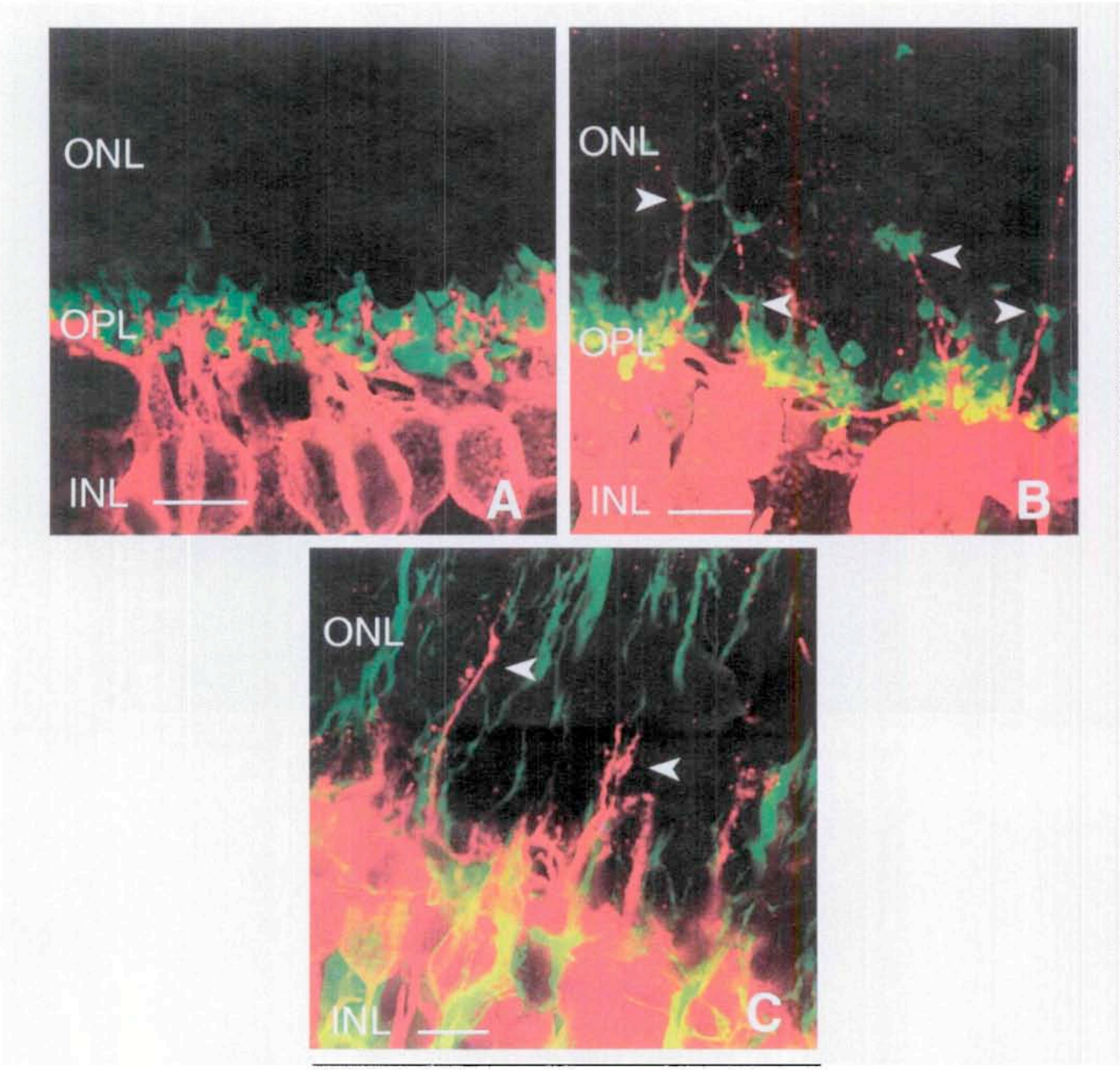

FIGURE 2. Double-label immunocytochemical analysis using antibodies to protein kinase C (PKC) (*red*) and either synaptophysin (**A**, **B**; *green*) or glial fibrillary acidic protein (GFAP) (**C**; *green*) of normal (**A**) and detached (**B**, **C**) retinal sections. (**A**) Normal retina. Anti-PKC labeling (*red*) is present in the cell bodies of the rod bipolars in the inner nuclear layer (*INL*) and their dendrites in the outer plexiform layer (*OPL*). Anti-synaptophysin labeling (*green*) is present in the rod and cone synaptic terminals. (**B**) 3-day retinal detachment. Anti-PKC-labeled rod bipolar dendrites (*red*) extend into the outer nuclear layer (*ONL*) in areas in which there is significant anti-synaptophysin labeling of retracted rod terminals (*green*; *arrowheads*). Note the disruption of anti-synaptophysin labeling that occurs in the OPL by comparison to **A**. (**C**) 28-day retinal detachment. One example of anti-PKC labeling (*red*) of the rod bipolar dendrites (*arrowheads*) that demonstrates that it is distinct from anti-GFAP labeling (*green*) within Müller cell processes in the ONL. **A**, a single image; **B**, a projection of 17 images; **C**, a projection of 12 images. *Bars*, 10 μm.

some amacrine cells (Fig. 3A). The processes of the calbindin-positive horizontal cells ramify into the OPL but not beyond. One day after detachment, fine, beaded, calbindin D-positive processes are present in the ONL (Fig. 3B). By day 28, these labeled neurites extend throughout the width of the ONL (Fig. 3C). No changes are observed in the inner retina or in cone cells after detachment.

Double labeling of normal retina with anti-synaptophysin and anti-calbindin D labels processes and photoreceptor synaptic terminals in the OPL (Fig. 4A). After detachment, calbindin D-positive processes lie among synaptophysin-positive terminals in the ONL (Fig. 4B). At higher magnification, anti-calbindin D-labeled processes can be seen to contact the anti-synaptophysin-labeled photoreceptor synaptic terminals in the ONL (Fig. 4C). These calbindin D-positive processes were not double labeled with anti-PDEγ, indicating that they are not derived from the cones (Fig. 4D). The calbindin D-positive processes also did not correspond to the anti-GFAP-labeled processes of Müller cells

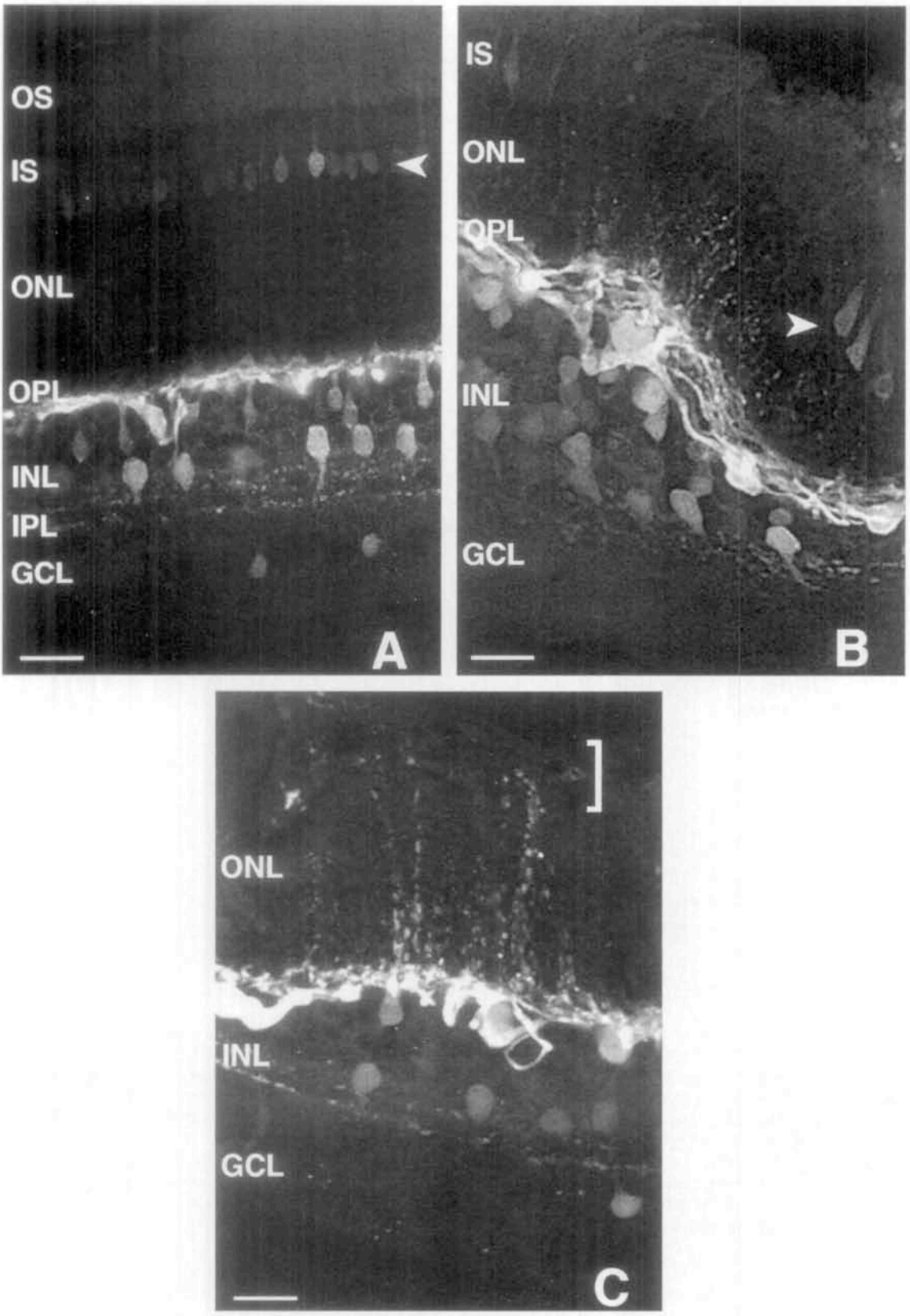

FIGURE 3. Anti-calbindin D labeling of normal (**A**) and detached (**B**, **C**) retinal sections. (**A**) Normal retina. The most intense labeling occurs in horizontal cell bodies in the inner nuclear layer (*INL*) and their processes in the outer plexiform layer (*OPL*). Labeling also occurs in the cone inner segments and cell bodies (*arrowheads*) at the outer edge of the outer nuclear layer (*ONL*), in the cone terminals in the OPL, in the amacrine cell bodies in the INL, in the amacrine cell processes in the inner plexiform layer (*IPL*), and in the cells in the ganglion cell layer (*GCL*). (**B**) 1-day retinal detachment. A slightly oblique plane of section demonstrates the intensely labeled network of horizontal cell processes running in the OPL and finer labeled horizontal cell processes extending into the ONL. (**C**) 28-day retinal detachment. Labeled processes extend past the inner segments (*IS*) into a subretinal glial scar (*bracket*). **A**, a single image; **B**, a projection of 12 images; **C**, a projection of 16 images. *Bars*, 20 μm.

(Figs. 4E, 4F; 28-day detachment). The long, anti-calbindin D-labeled processes appeared most frequently in areas in which there was extensive anti-GFAP labeling, that is, significant Müller cell hypertrophy (Figs. 4E, 4F). In some cases, anti-calbindin D-labeled processes were observed among GFAP-positive Müller cell processes extending past the photoreceptor outer segments into the subretinal space (Fig. 4F).

Electron Microscopic Analysis

The OPL undergoes dramatic reorganization after detachment. Normally, the OPL is highly organized with a layer of rod and cone terminals tightly packed together (Fig. 5A). After detachment, many rod terminals retract from the OPL and are found throughout the ONL (Figs. 5B, 5C). These terminals have an altered morphology but still contain synaptic ribbons. In many cases, ribbons and synaptic contacts are present in photoreceptor cell bodies in the ONL (Figs. 5B, 5C). Occasionally, these photoreceptor synapses contact processes with an electron-lucent morphology resembling that of rod bipolar cell dendrites (Fig. 5C).[9] Increased numbers of vesicle-containing photoreceptor processes are also found in the ONL (Fig. 6A) that are synaptophysin positive (Figs. 6B, 6C). Cone terminals, however, are not found within the ONL after detachment but remain in the OPL, assuming a flattened appearance and losing their deep synaptic invaginations (data not shown).[3] Based on ultrastructural observations, the anti-synaptophysin labeling in the ONL seen by confocal microscopy most likely represents both labeling of synaptic vesicles in retracted rod synaptic terminals and labeling of the clusters of vesicles in photoreceptor axons crossing the ONL.

Discussion

Results from this study provide new information on retinal detachment and add to earlier conclusions about changes in the photoreceptor cells, their synaptic terminals, and second-order neurons after detachment. Previously[3] we noted that photoreceptor terminals lost their deep synaptic invaginations, became vacuolated, had reduced numbers of synaptic vesicles, and, in the case of rods, often withdrew their axons so that synaptic structures were found in rod cell bodies in the ONL. Whereas our earlier emphasis was on degenerative changes in the synaptic terminals,[3,10] these recent observations suggest that the structural changes in the terminals, like those associated with the outer segment,[5] may represent a mechanism that allows these cells to survive and recover from a brief period of detachment.[11] Similarly, the neurite outgrowth from second-order neurons, as described here, may help to assure the integrity of the various pathways between photoreceptors and the inner retina during such a period of detachment.

With the use of antibody labeling and confocal microscopic analysis, we found structural changes in photoreceptor terminals, especially those of the rods, within 1 day of detachment. These changes include the loss of the normal shape of individual rod spherules, the overall disrupted appearance of the layer of spherules, and the appearance of anti-synaptophysin labeling deep in the ONL. They are correlated with ultrastructural observations of synaptic ribbons and vesicles deep in the ONL, the loss of deep synaptic invaginations in the rod spherules, and a decrease in their synaptic vesicle content. The changes for anti-synaptophysin labeling closely parallels the ultrastructural changes in rod spherule morphology, whereas the changes, reported in an earlier study, in the labeling pattern for tubulin and F-actin do not.[10] In these cases, the labeling simply disappears from the synaptic terminals over the course of a few days. The overall shape changes and the loss of synaptic invaginations in rod and cone terminals may, in fact, result from the loss of the cortical F-actin cytoskeleton after detachment. Concurrently, the clusters of anti-synaptophysin-labeled vesicles that occur along the photoreceptor axons in the mid-ONL, a phenomenon uncommon in normal retina, combined with the reduction of terminal vesicles, may be a result of the loss of microtubules because these organelles are commonly associated with vesicular transport.[12]

Based on the ultrastructural appearance of processes in the OPL, we speculated in our earlier study that transneuronal degeneration of cells in the INL may occur as a result of the loss of photoreceptor synaptic contact.[3] This does not appear to be the case. Although an occasional cell body in the INL may show indications of degeneration, it is rarely encountered, and Cook et al.[4] did not find terminal deoxynucleotidyl transferase-mediated dUTP nick end labeling (TUNEL) (apoptotic) cells in the INL between 1 and 28 days after detachment. In fact, the major response of the second-order neurons to retinal detachment appears to be the growth of elongated processes into the ONL as described here.

The use of anti-PKC and anti-calbindin D as labels for rod bipolar cells and horizontal cells, respectively, revealed rapid outgrowth of their processes after detachment. It seems likely that these outgrowths reflect the various changes occurring in the photoreceptor cell population. In normal retina, rod bipolar and horizontal cell processes terminate as a band in the OPL. Within 1 day of detachment (when anti-synaptophysin-labeled synaptic terminals appear in the ONL), rod bipolar and horizontal-cell processes extend into the ONL. With time, these extended processes become longer and more numerous. They frequently adjoin anti-synaptophysin-labeled profiles deep in the ONL; by electron microscopic analysis, the synaptic ribbon synapses deep in the ONL usually contact postsynaptic processes that resemble dendrites of rod bipolar cells. This change may indicate significant remodeling of the rod bipolar cell dendritic trees and B-type, horizontal-cell axon-terminal arborization in response to detachment.

The growth and shrinkage of adult neuronal dendritic trees have been reported to occur in the central nervous system after deafferentiation,[13] axotomy,[14] cortical lesions,[15-17] self-stimulation,[18] neurotrophin infusion,[19-21] drug infusion,[22-24] during motor learning,[25] trytophan deprivation,[26] aging,[27,28] and Huntington disease.[29] Reports of similar changes in retinal neurons have been extremely limited. Neurite sprouting, also documented by anti-calbindin D labeling, was found in horizontal cells in the late stages of photoreceptor degeneration in the Royal College of Surgeons rat.[30] In a report describing rod neurite sprouting in late-stage retinitis pigmentosa, Li et al.[31] indicate that, "a few (calbindin D) labeled horizontal-cell processes gave rise to abnormal apical sprouts." In cat and rabbit retinas treated with kainic acid, horizontal cells are reported first to shrink and then to form and extend abnormal processes into the inner retina.[32] In contrast, the neurite outgrowths we observed did not occur after massive photoreceptor cell death (as in the Royal College of Surgeons rat and retinitis pigmentosa), nor did they grow into the inner retina. In fact, they occurred in regions in which the ONL is thinned by photoreceptor death and in regions of near-normal thickness. The rod bipolar and horizontal cells'

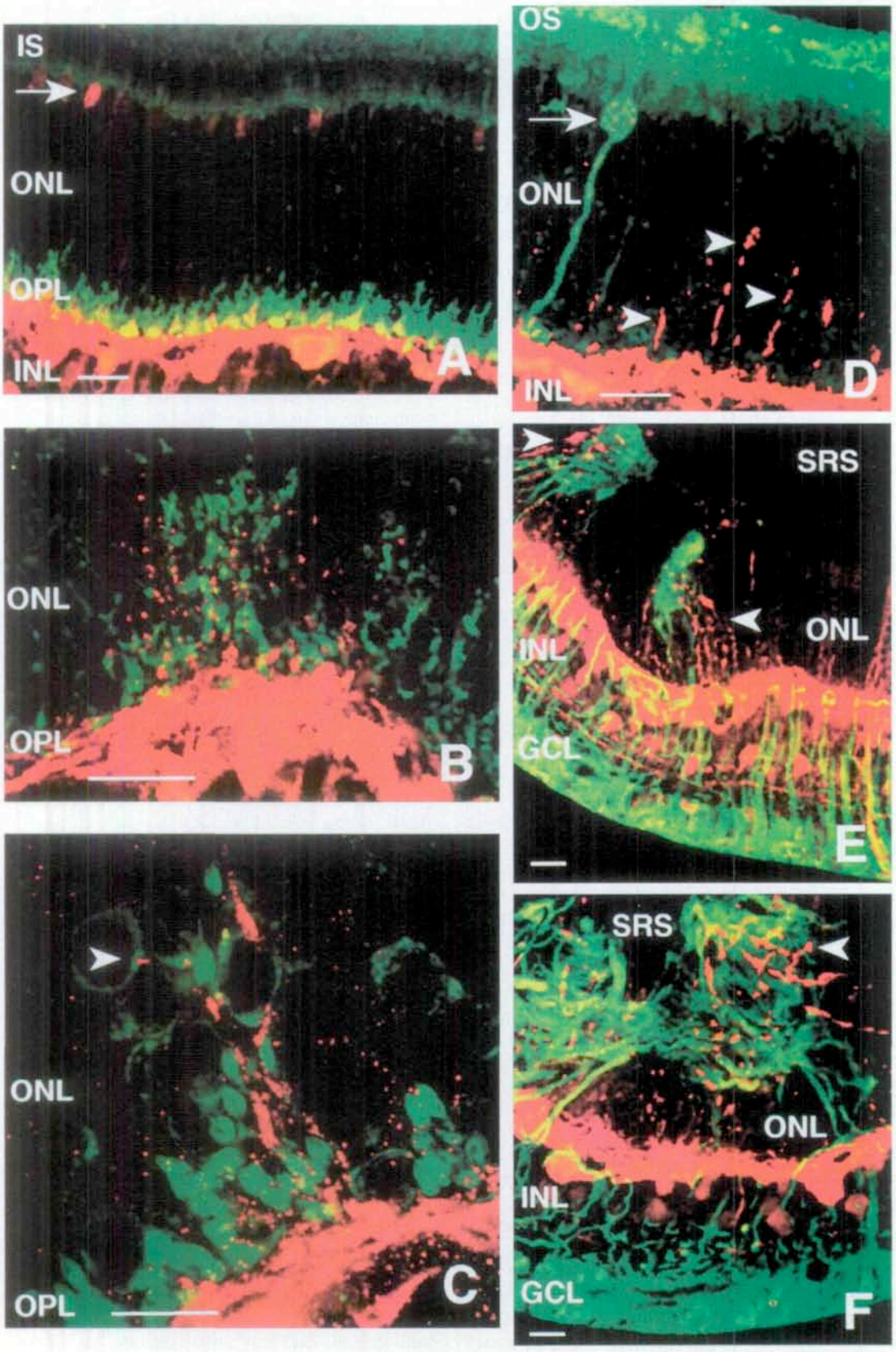

FIGURE 4. Double-label immunocytochemical analysis using antibodies to calbindin D (*red*) and either synaptophysin (**A**, **B**, **C**; *green*), phosphodiesterase γ (PDEγ; **D**; *green*), or anti-glial fibrillary acidic protein (GFAP, **E**, **F**; *green*) of normal (**A**) and detached (**B**–**F**) retinal sections. (**A**) Normal retina. Anti-calbindin D labeling (*red*) is present in horizontal cells (HC) in the inner nuclear layer (*INL*) and in cone cell bodies (*arrow*) and cone synaptic terminals in the outer plexiform layer (*OPL*). Anti-synaptophysin labeling (*green*) is present in the rod and cone synaptic terminals. The cone terminals appear *yellow* because of the colocalization of synaptophysin and calbindin D. (**B**) 1-day retinal detachment. Anti-calbindin labeling (*red*)

FIGURE 4 *(Continued).* in the outer nuclear layer (*ONL*) occurs in areas in which there is significant anti-synaptophysin labeling (*green*). Note the reduction of anti-synaptophysin labeling in the disrupted OPL. (**C**) 28-day retinal detachment. An anti-calbindin D-labeled process (*red*) can be seen contacting a synaptophysin-positive photoreceptor terminal (*green*) that has retracted into the cell body (*arrowhead*). (**D**) 28-day detached retina. Anti-PDEγ labeling (*green*) occurs only in the cones (*arrow*) and the outer segments (*OS*); no PDEγ labeling is present in the horizontal cell processes (*red*; *arrowheads*) extending into the ONL. (**E**) 28-day detached retina. Anti-calbindin D labeling of HC processes (*red*; *arrowheads*) within the ONL does not colocalize with the anti-GFAP-labeled Müller cell processes (*green*). Note, however, that some HC outgrowths appear to extend to regions in which there is significant anti-GFAP labeling. (**F**) 28-day detached retina. Anti-calbindin D-labeled HC processes (*red*) lie among hypertrophied Müller cell processes, which are labeled with anti-GFAP (*green*; *arrowheads*) in the subretinal space (*SRS*). A projection of (**A**) 6 images; (**B**, **C**, **D**), 10 images; (**E**), 8 images; (**F**), 14 images. *Bars*, 20 μm (**A**, **B**, **D**, **E**, **F**); 10 μm (**C**).

neurites are always directed into the ONL, often ending near an anti-synaptophysin-labeled photoreceptor synapse. Thus, in our model, the second-order neurons responded rapidly to relatively subtle changes in the photoreceptor cell population. The timing of neurite outgrowth observed here is similar to that reported to occur in the ciliary ganglion after axotomy[14] and in dentate granule cells after cortical lesioning.[16]

Several questions arise from the results presented here: Does neurite sprouting occur in human retinal detachment? Does the response occur in the cone as well as the rod pathway? What are the functional implications, if any? What stimulates neurite outgrowth?

Regarding the first question, obtaining fixed tissue from short-term detachments is difficult, because enucleation rarely occurs after uncomplicated reattachment surgery. It seems likely that neurite sprouting does occur in human detachments, because other events identified in animal models occur in humans (for example, outer segment degeneration and pho-

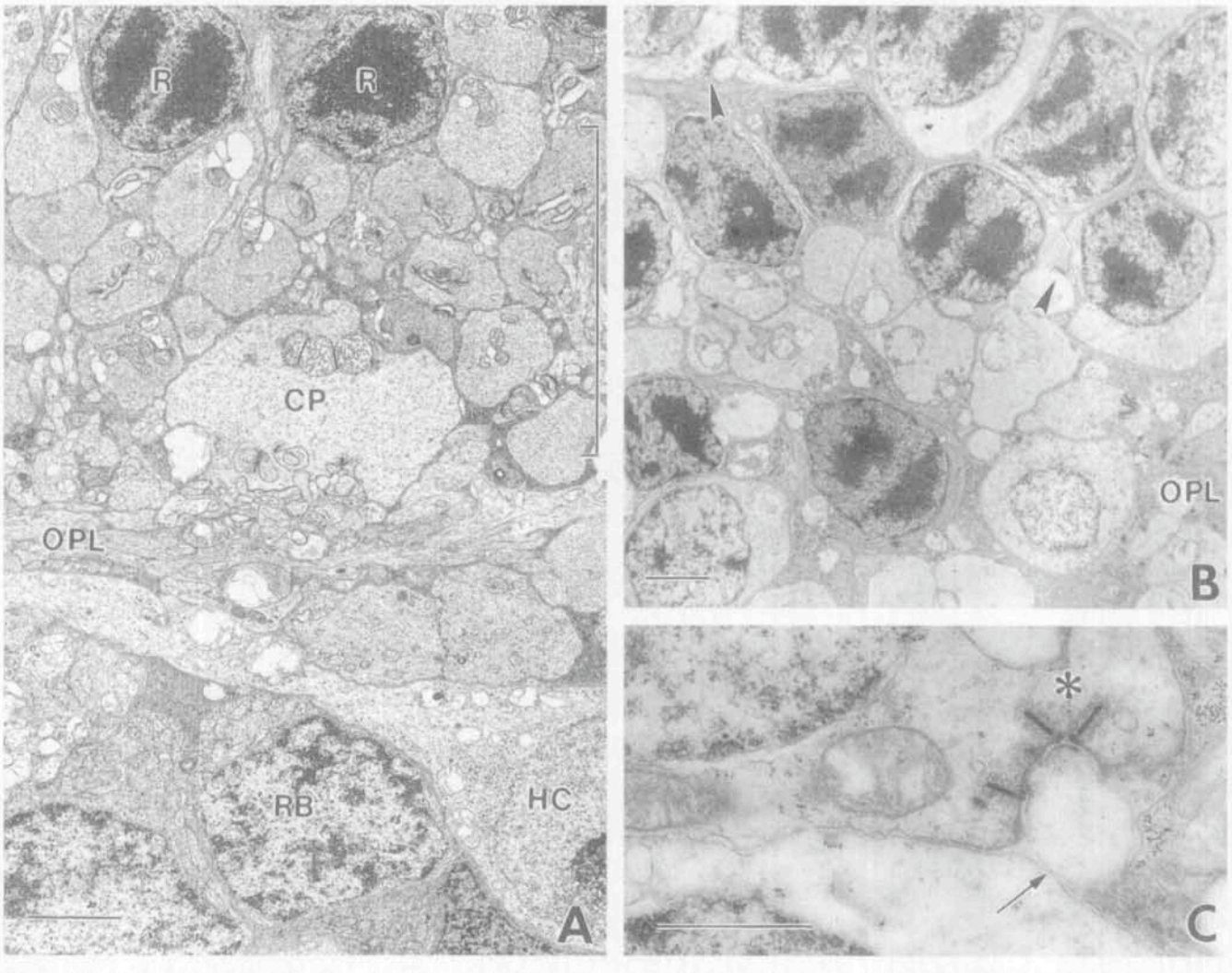

FIGURE 5. Electron micrographs showing changes in the outer retina after detachment. (**A**) Normal retina showing an organized outer plexiform layer (*OPL*) with rod and cone (*CP*) terminals. The *bracket* indicates the rod terminal zone. (**B**) 28-day detachment showing a disrupted OPL with several rod terminals (*arrowheads*) adjacent to their cell bodies. (**C**) 28-day detachment showing a higher magnification of a rod terminal (*) in the mid-outer nuclear layer contacting a presumed bipolar cell dendrite (*arrow*). Note the shallow invagination in the rod terminal. *R*, rod photoreceptor cell; *RB*, rod bipolar cell; *HC*, horizontal cell. *Bars*, 2 μm (**A**, **B**); 1 μm (**C**).

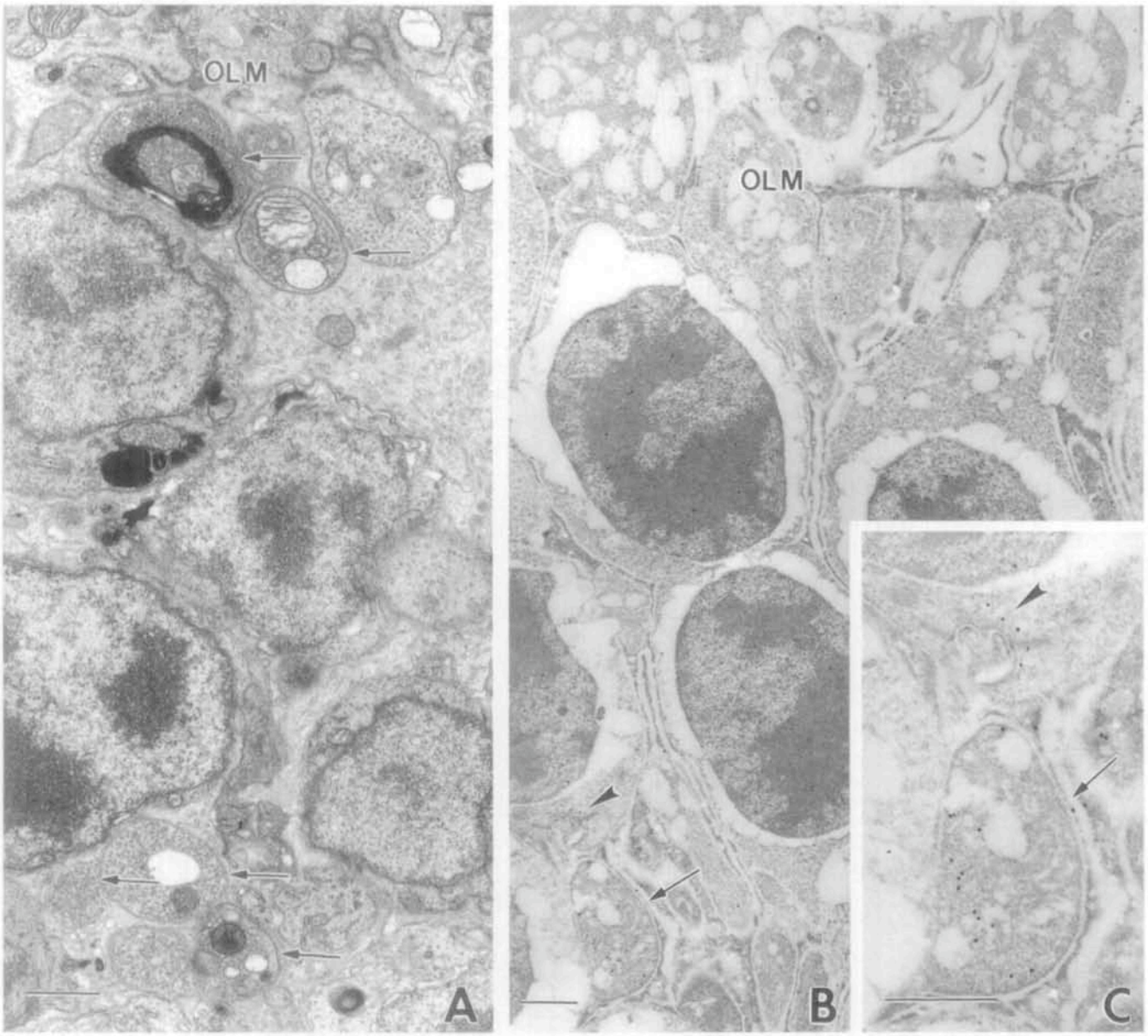

FIGURE 6. Electron micrographs showing changes in the outer retina after detachment. (**A**) 2-day detachment showing vesicle-filled processes (*arrows*) near the outer limiting membrane (*OLM*). (**B**) 7-day detachment immunolabeled with anti-synaptophysin. Gold spheres are present in a rod terminal (*arrow*) adjacent to a photoreceptor cell body (*arrowhead*). (**C**) Higher magnification of the rod terminal and process labeled with anti-synaptophysin. *Bars*, 1 μm.

toreceptor cell death[33-36] and gliosis[36-38]). The most direct answer to the second question will come from the discovery of specific markers for cone bipolar cells, but in their absence, evidence could also come from studies on detachments involving the fovea or cone-dominant retinas. An answer to the third question requires specific physiological studies. In terms of overall visual consequences, the growth of neurites may represent a mechanism for maintaining the integrity of the rod pathway. Because the rod pathway is highly redundant, the new neurites may assure that remaining rods retain connections to the inner retina and, therefore, preserve the portion of the rod system that survives the cell death induced by detachment. Maintenance of connections between rods and second-order neurons may promote recovery of vision on retinal reattachment and assure the survival of second-order neurons and rods, assuming a trophic relationship between the two cell types. Understanding the stimulus for neurite outgrowth (the fourth question above) may have broader implications for understanding retinal development and development of therapy for photoreceptor diseases. In general, neurite outgrowth is a response to trophic factors, for example, nerve growth factor.[39] Exactly which molecules stimulate neurite sprouting by rod bipolar cells and horizontal cells is difficult to predict, because little is known about trophic factors released by retinal cells. There is evidence that basic fibroblast growth factor (bFGF) is produced by photoreceptors,[40-43] and there are binding sites for this factor within the synaptic invaginations of photoreceptors.[44] If these binding sites represent receptors on the dendrites of rod bipolar cells and horizontal cells, then it is possible that neurites form in response to the release of bFGF from the photoreceptor terminals as they retract from the OPL. However, there are other factors identified in the retina, in-

cluding brain-derived neurotrophic factor,[42,45] neurotrophin-3,[46] ciliary neurotrophic factor,[42,47] insulin-like growth factor,[42,48] retinoic acid,[49] and acidic fibroblast growth factor,[50] that may fulfill this role.

There is also the question of whether reattachment and photoreceptor recovery involves a reversal of the events described here or whether the new structural configurations assumed by the synaptic terminals and processes from second-order neurons simply remain intact. If the latter is the case, what effect might this have on the recovery of vision? Are any of the visual deficits that remain after successful reattachment surgery attributable to these changes?

Transplantation of the entire photoreceptor layer has been proposed as a therapy for diseases such as retinitis pigmentosa.[51-53] Success in such ventures would depend on the formation of connections between transplanted photoreceptors and the second-order host neurons. Our data suggest that such second-order neurons have the potential to grow processes that could connect to the photoreceptors. It is unknown whether they retain this potential after extended photoreceptor degeneration, such as occurs in retinitis pigmentosa, or whether their connections reform a functional visual pathway. In contrast, the events we have identified occur quickly, when the photoreceptor layer remains relatively intact and the photoreceptor terminals still contact processes of their postsynaptic cells.

In summary, the ability of the second-order neurons in the retina to sprout neurites quickly may have implications for the survival of these cells during photoreceptor degeneration. It also may be a way of assuring the integrity of the visual pathway during an episode of retinal detachment and of promoting recovery on reattachment.

Acknowledgments

The authors thank Cherlin Johnson, Jared Younger, and Rick Hussey for their technical assistance.

References

1. Bok D. Retinal photoreceptor-pigment epithelium interactions. *Invest Ophthalmol Vis Sci.* 1985;26:1659-1693.
2. Fisher SK, Anderson DH. Cellular effects of retinal detachment on the neural retina and the retinal pigment epithelium. In: Glaser BM, Michels RG, eds. *Retina.* St. Louis, MO: CV Mosby;1989:165-190.
3. Erickson PA, Fisher SK, Anderson DH, Stern WH, Borgula GA. Retinal detachment in the cat: the outer nuclear and outer plexiform layers. *Invest Ophthalmol Vis Sci.* 1983;24:927-942.
4. Cook B, Lewis GP, Fisher SK, Adler R. Apoptotic photoreceptor degeneration in experimental retinal detachment. *Invest Ophthalmol Vis Sci.* 1995;36:990-996.
5. Anderson DH, Guerin CJ, Erickson PA, Stern WH, Fisher SK. Morphological recovery in the reattached retina. *Invest Ophthalmol Vis Sci.* 1986;27:168-183.
6. Matsumoto B, Hale IL. Preparation of retinas for studying photoreceptors with confocal microscopy. *Methods Neurosci.* 1993;15:54-71.
7. Fisher SK, Anderson DH, Erickson PA, Guerin CJ, Lewis GP, Linberg KA. Light and electron microscopy of vertebrate photoreceptors. *Methods Neurosci.* 1993;15:3-36.
8. Erickson PA, Anderson DH, Fisher SK. Use of uranyl acetate *en bloc* to improve tissue preservation and labeling for post-embedding immunoelectron microscopy. *J Electron Microsc Tech.* 1987;5:303-314.
9. Linberg KA, Fisher SK. Ultrastructural evidence that horizontal cell axon terminals are presynaptic in the human retina. *J Comp Neurol.* 1988;268:281-297.
10. Lewis GP, Matsumoto B, Fisher SK. Changes in the organization and expression of cytoskeletal proteins during retinal degeneration induced by retinal detachment. *Invest Ophthalmol Vis Sci.* 1995;36:2404-2416.
11. Fariss RN, Molday RS, Fisher SK, Matsumoto B. Evidence from normal and degenerating photoreceptors that two outer segment integral membrane proteins have separate transport pathways. *J Comp Neurol.* 1997;387:148-156.
12. Vale R. Intracellular transport using microtubule-based motors. *Ann Rev Cell Biol.* 1987;3:347-378.
13. Strata P, Tempia F, Zagrebelsky M, Rossi F. Reciprocal trophic interactions between climbing fibres and Purkinje cells in the rat cerebellum. *Prog Brain Res.* 1997;114:263-282.
14. Zhang YL, Tan CK, Wong WC. Electron microscopic study of sprouting dendrites in the ciliary ganglia of cat and monkey (*Macaca fascicularis*) following pre- and post-ganglionic axotomy. *Histol Histopathol.* 1997;12:1-8.
15. Jones TA, Kleim JA, Greenough WT. Synaptogenesis and dendritic growth in the cortex opposite unilateral sensorimotor cortex damage in adult rats: a quantitative electron microscopic examination. *Brain Res.* 1996;733:142-148.
16. Schauwecker PE, McNeill TH. Dendritic remodeling of dentate granule cells following a combined entorhinal cortex/fimbria fornix lesion. *Exp Neuro.* 1996;141:145-153.
17. Kolb B, Ladowski R, Gibb R, Gorny G. Does dendritic growth underlie recovery from neonatal occipital lesions in rats? *Behav Brain Res.* 1996;77:125-133.
18. Rao BS, Desiraju T, Raju TR. Neuronal plasticity induced by self-stimulation rewarding experience in rats: a study on alteration in dendritic branching in pyramidal neurons of hippocampus and motor cortex. *Brain Res.* 1993;627:216-224.
19. Kolb B, Gorny G, Cote S, Ribeiro-da-Silva A, Cuello AC. Nerve growth factor stimulates growth of cortical pyrmidal neurons in young adult rats. *Brain Res.* 1997;751:289-294.
20. Tseng JL, Baetge EE, Zurn AD, Aebisher P. GDNF reduces drug-induced rotational behaviour after medial forebrain bundle transection by a mechanism not involving striatal dopamine. *J Neurosci.* 1997;17:325-333.
21. Andrews TJ, Cowen T. Nerve growth factor enhances the dendritic arborization of sympathetic ganglion cells undergoing atrophy in aged rats. *J Neurocytol.* 1994;23:234-241.
22. Dawirs RR, Teuchert-Noodt G, Nossoll M. Pharmacologically induced neural plasticity in the prefrontal cortex of adult gerbils (*Meriones unguiculatus*). *Eur J Pharmacol.* 1997;327:117-123.
23. Suzuki F, Makiura Y, Guilhem D, Sorensen JC, Onteniente B. Correlated axonal sprouting and dendritic spine formation during kainate-induce neuronal morphogenesis in the dentate gyrus of adult mice. *Exp Neurol.* 1997;145:203-213.
24. Suzuki F, Junier MP, Guilhem D, Sorensen JC, Onteniente B. Morphogenetic effect of kainate on adult hippocampal neurons associated with a prolonged expression of brain-derived neurotrophic factor. *Neuroscience.* 1995;64:665-674.
25. Kleim JA, Swain RA, Czerlanix CM, Kelly JL, Pipitone MA, Greenough WT. Learning-dependent dendritic hypertrophy of cerebellar stellate cells: plasticity of local circuit neurons. *Neurobiol Learn Mem.* 1997;67:29-33.
26. Gonzalez-Burgos I, del Angel-Meza AR, Barajas-Lopez G, Feria-Velasco A. Tryptophan restriction causes long-term plastic changes in corticofrontal pyramidal neurons. *Int J Dev Neurosci.* 1996;14:673-679.
27. Pyapali GK, Turner DA. Increased dendritic extent in hippocampal CA1 neurons from aged F344 rats. *Neurobiol Aging.* 1996;17:601-611.
28. Wellman CL, Sengelaub DR. Alterations in dendritic morphology of frontal cortical neurons after basal forbrain lesions in adult and aged rats. *Brain Res.* 1995;669:48-58.
29. Sotrel A, Williams RS, Kaufmann WE, Myers RH. Evidence for neuronal degeneration and dendritic plasticity in cortical pyramidal neurons of Huntington's disease: a quantitative Golgi study. *Neurology.* 1993;43:2088-2096.
30. Chu Y, Humphrey MF, Constable IJ. Horizontal cells of the normal and dystrophic rat retina: a whole mount study using immunolabelling for the 28-kDa calcium binding protein. *Exp Eye Res.* 1993;57:141-148.
31. Li ZY, Kljavin IJ, Milam AH. Rod photoreceptor neurite sprouting in retinitis pigmentosa. *J Neurosci.* 1995;15:5429-5438.

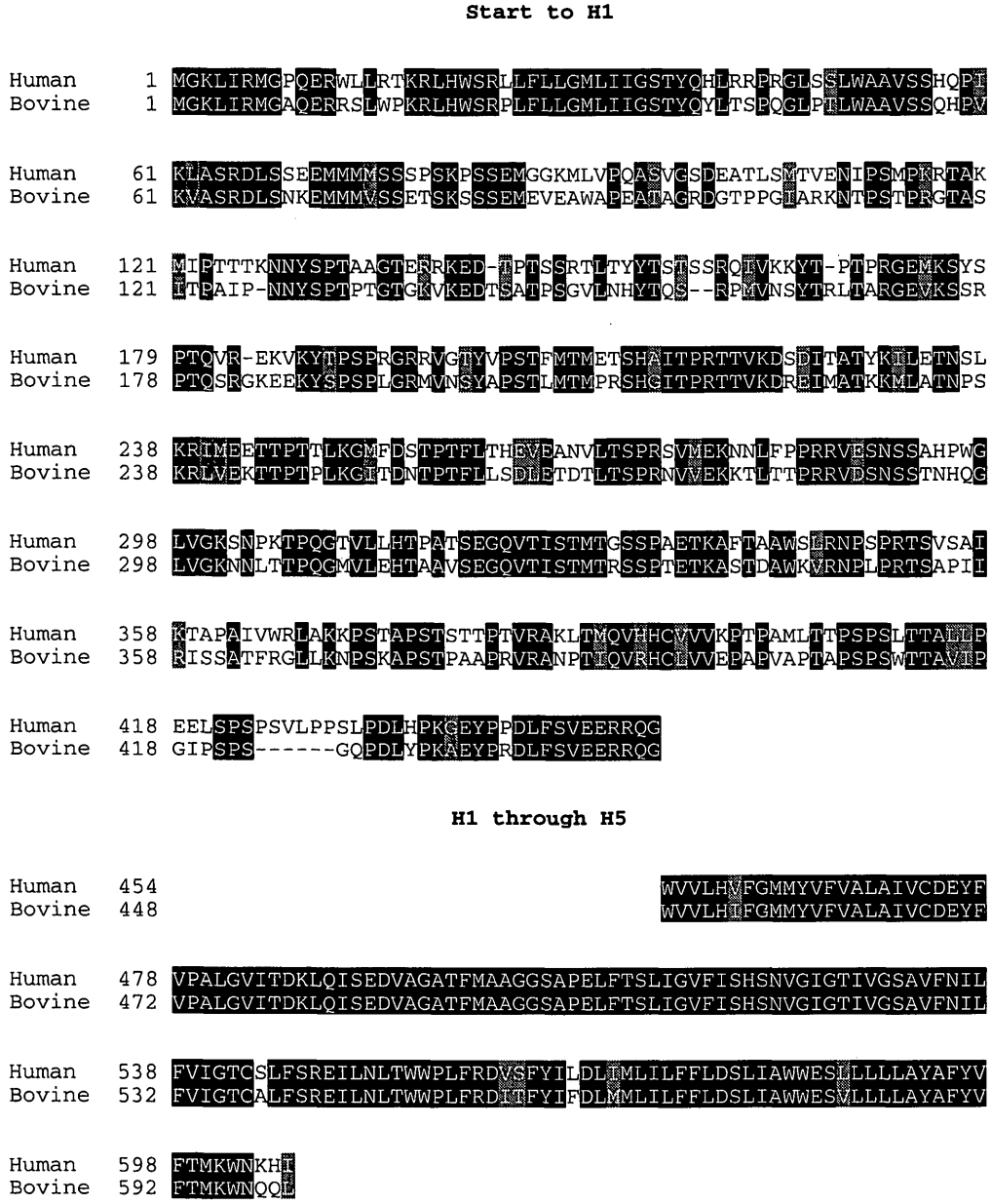

FIGURE 1. Comparison between the deduced amino acid sequences of the human and bovine retinal rod Na-Ca+K exchangers. This is the revised sequence of the bovine cDNA that we obtained (see text and Fig. 3). *Black-shaded* residues indicate identity, whereas *gray-shaded* residues indicate conservative substitutions.

distinct clones. Inserts from each of the 12 isolated exchanger clones were amplified directly from lambda clones using standard lambda gt10 forward and reverse primers and were sequenced with those same primers. Further primers were based on the sequences thus obtained. Sequences were determined by standard automated (ABI 373A; Applied Biosystems, Foster City, CA) and manual (dsDNA Cycle; BRL, Burlington, Ontario) sequencing protocols.

Construction and Sequencing of Buffalo and Bovine Retinal Na-Ca+K Exchanger cDNA

Bovine and buffalo retinas were dissected from freshly obtained eyeballs and were frozen at −75°C for future use. Total RNA was isolated from frozen retinas with Trizol Reagent (Gibco BRL, Burlington, Ontario, Canada) according to the manufacturer's instructions. PolyA$^+$ RNA was isolated on New England Biolabs oligo(dT) cellulose spin columns (Mississauga, Ontario, Canada) according to the manufacturer's instructions. The forward primers, 5′CAGACGTCAAGGGAGATCAGGAGG3′ and 5′CCATCCACACCTTCCTCGTCATC3′, and the reverse primers, 5′CCNTC(T/C)TG(G/A)TGNGCACCA3′ and 5′TCCCGGCAGAAAGGAGAGGAGATG3′, were synthesized to flank the cytosolic region of the exchanger, based on the published bovine NCKX sequence. Single-stranded cDNAs were generated by using reverse transcription (Superscript II; Gibco BRL) with the use of random hexamer primers according to the manufacturer's instructions. Using the above primers, PCR fragments from our buffalo and bovine cDNA clones, as well as from a previously cloned bovine cDNA,[6] were synthesized, isolated, and used for generating overlapping nucle-

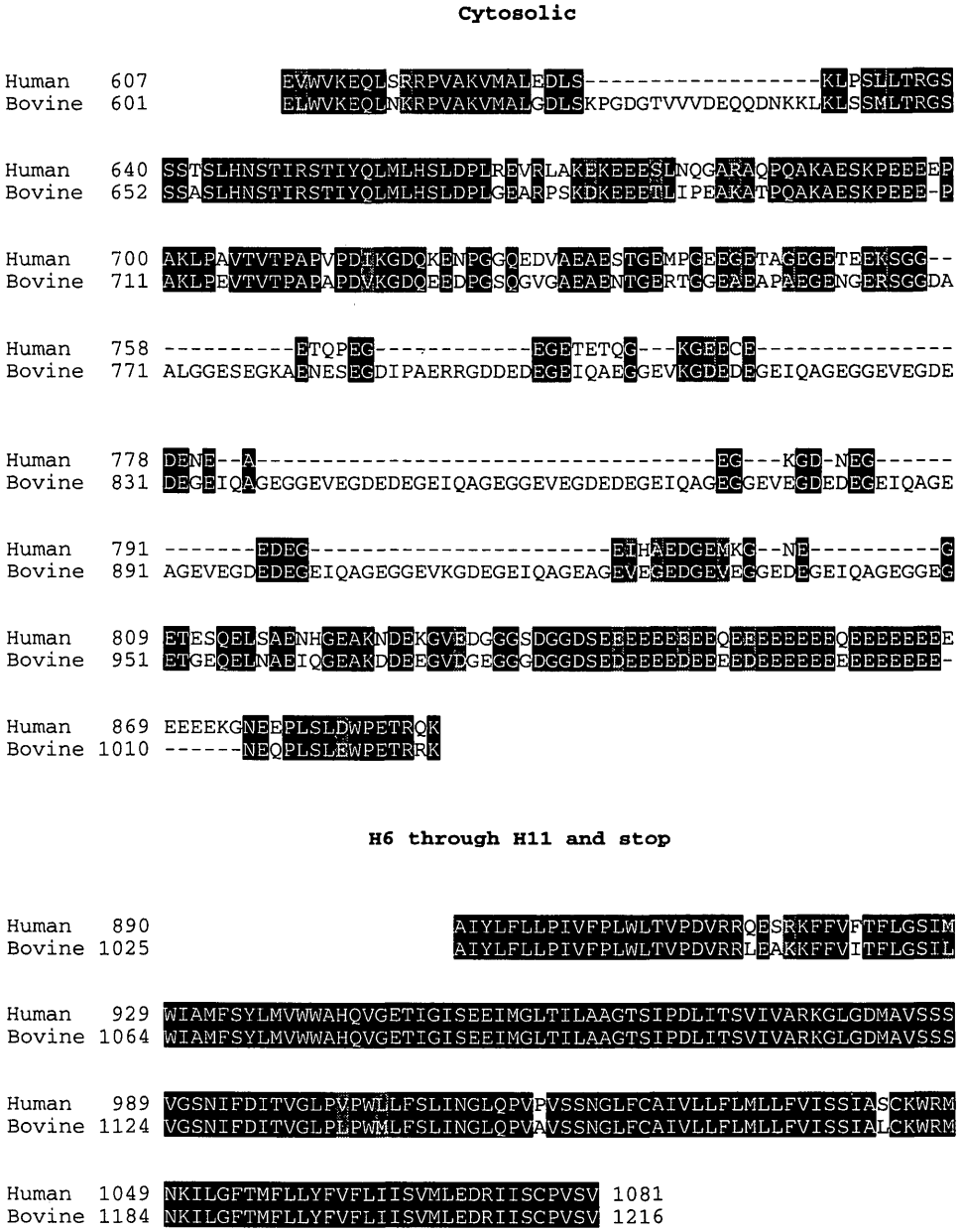

FIGURE 1 *(Continued)*

otide sequences from part of the cytosolic loop that includes the repeat region. Sequences were confirmed by correlating *Alu*I restriction maps with the number of nucleotides between *Alu*I sites read on the sequences obtained.

RESULTS

Cloning the Human Retinal Rod Na-Ca+K Exchanger

We screened a human retinal cDNA library for clones that showed homology with the bovine retinal rod Na-Ca+K exchanger. Twelve positive clones were analyzed, all of which contained sequences homologous to the bovine rod Na-Ca+K exchanger cDNA and from which the entire coding sequence was obtained. In all cases, overlapping sequences between different cDNA clones of the human exchanger were identical, indicating that all clones represented a single cDNA species. The deduced amino acid sequence of the human rod Na-Ca+K exchanger resulted in a protein of 1081 amino acids, 135 amino acids shorter than our revised sequence of the bovine rod Na-Ca+K exchanger. The comparison of the deduced amino acid sequence of the human Na-Ca+K exchanger with that of the bovine rod Na-Ca+K exchanger as revised by us (see below) is illustrated in Figure 1. Sequence comparison suggests an identical topology for both exchangers, with four distinct domains within the entire Na-Ca+K exchanger sequence (Fig. 2), and yields an overall identity of 64.3% at the amino acid level between the bovine and human rod Na-Ca+K exchangers. The greatest degree of identity is observed between the two sets of putative transmembrane-spanning domains and their short connecting loops: 94% for H1 through H5, and 95% for H6 through H11. Identity or, in one case, a conservative substitution was observed for all charged residues within the putative transmembrane-spanning domains. The extracellular loop was poorly conserved, with only 59% overall

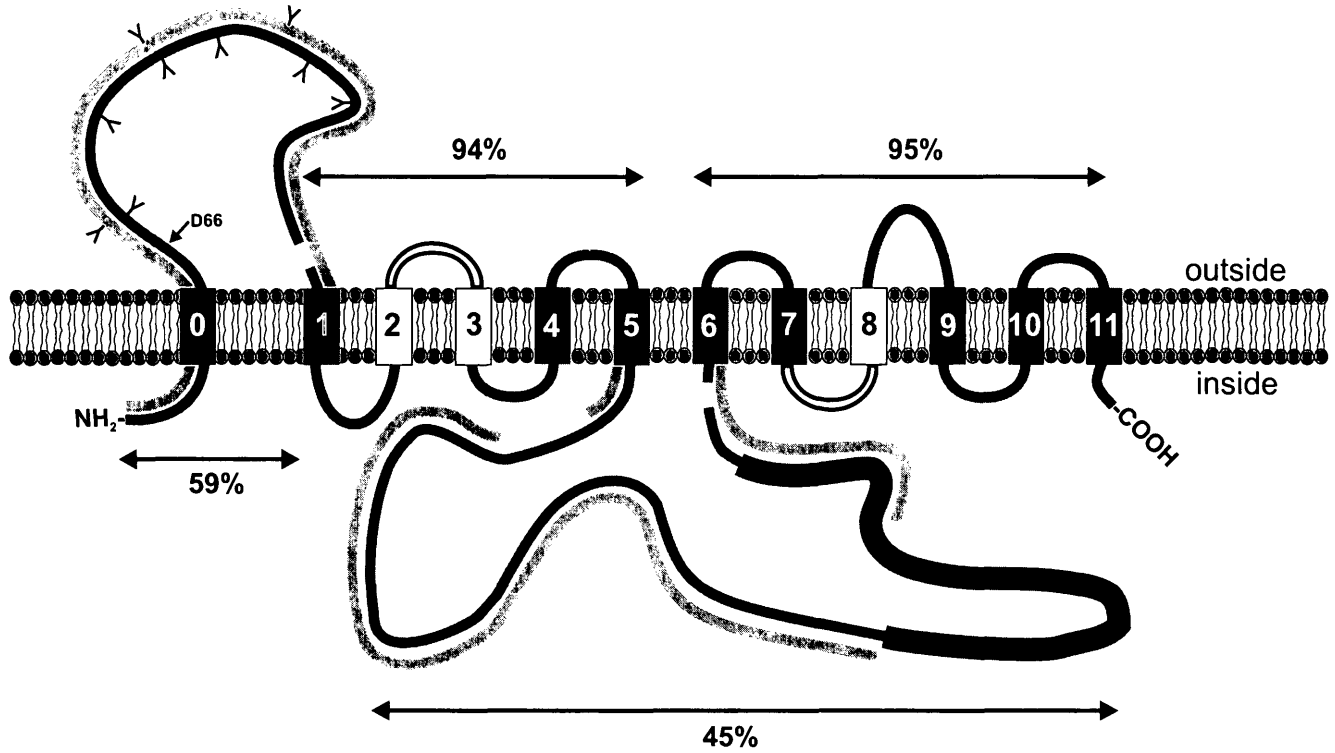

FIGURE 2. The bovine-human rod Na-Ca+K exchanger. Diagram of the putative topology of the bovine (*black*) and human (*gray*) rod outer segment (ROS) Na-Ca+K exchangers. Possible glycosylation sites (*Y*) are indicated only in the extracellular loop. D66 represents the N terminus of the exchanger purified from bovine ROS. For cases in which one of the two sequences shows a deletion about the other, gaps are shown. The *open boxes* of transmembrane-spanning domains *2*, *3*, and *8* with their connecting loops (*2-3*, *7-8*) represent the only areas with sequence similarity to the NCX1 clones. The *thickened portion* of the bovine cytosolic loop marks the position of the repeats dominated by acidic amino acid residues. Percentages indicate sequence identity in the respective domains.

identity, although the length was similar in both sequences (the major exception is a six-amino acid insertion observed in the human sequence after residue 423). H0 as well as the sequence around the proposed cleavage site at D66 were relatively well conserved. The native bovine Na-Ca+K exchanger is heavily glycosylated,[10] and the extracellular loop of the bovine exchanger contains six possible glycosylation sites. Of the six glycosylation sites, two are conserved in the human rod exchanger (at positions 129 and 290, respectively) and four are lost, whereas one new site is observed (at residue 347). Finally, the large cytosolic loop between the transmembrane-spanning domains H5 and H6 shows only 45% identity between the human and bovine sequences, in part caused by two deletions. First, at amino acid 629 in the human exchanger sequence, a drop out of 18 amino acids was observed (as obtained from two separate clones). Second, the bovine exchanger sequence contains several repeats of a 17-amino acid motif that was not observed in the human sequence (obtained from three separate clones; see also below and Fig. 3). Both the human and the bovine rod Na-Ca+K exchangers have a long stretch of approximately 30 glutamic acid residues immediately adjacent to H6. In this case, the bovine sequence (at residue 1009) shows a dropout of seven amino acids compared to the human sequence.

Partial Cloning and Sequencing of Bovine and Buffalo Na-Ca+K Exchanger cDNA Clones

Unlike the NCX cDNAs, the rod Na-Ca+K exchanger seems to have at least two large, poorly conserved domains, and we were particularly intrigued about the presence (bovine) or absence (human) of a series of repeats of a stretch of mostly acidic amino acids located in the putative large cytosolic loop. To address the issue of these repeats in more detail, we obtained a partial sequence from a buffalo retinal rod Na-Ca+K exchanger clone, and we examined the same stretch in the sequence of the bottlenosed dolphin (*Tursiops*) retinal rod Na-Ca+K exchanger that we had cloned in our laboratory. The buffalo sequence was obtained from PCR fragments isolated by using primers that flank the area of interest on first-strand cDNA synthesized from buffalo retinal polyA$^+$ RNA. In this experiment, we ran, as a control, the same PCR fragment obtained from bovine retinal polyA$^+$ RNA, and we noted a significant difference in size between the bovine and buffalo sequences measuring approximately 100 nucleotides. The buffalo fragment was sequenced, and it was discovered to be 51 nucleotides shorter when compared with the published bovine sequence.[6] Hence, we obtained the same PCR fragment using the published bovine rod Na-Ca+K exchanger clone as a template. The fragment proved to be identical in size to that fragment isolated from our bovine cDNA (synthesized from polyA$^+$ RNA), suggesting a discrepancy between the published cDNA sequence and the actual sequence of the bovine Na-Ca+K exchanger clones. Sequencing of the PCR fragments showed that the bovine sequence contains a glycine as residue 857 rather than the alanine residue in the published sequence and that it contains an additional full repeat. Thus, the cDNA of the bovine exchanger codes for 9 rather than 8 of the 17 amino acid repeats, resulting in an insert of DEDEGEIQAGEGGEVEG between residues 862 and 863 of the published sequence.[6]

Figure 3 illustrates for the different species the alignment of the sequences that correspond to the area of the acidic repeats found in the bovine sequence. The buffalo sequence showed that

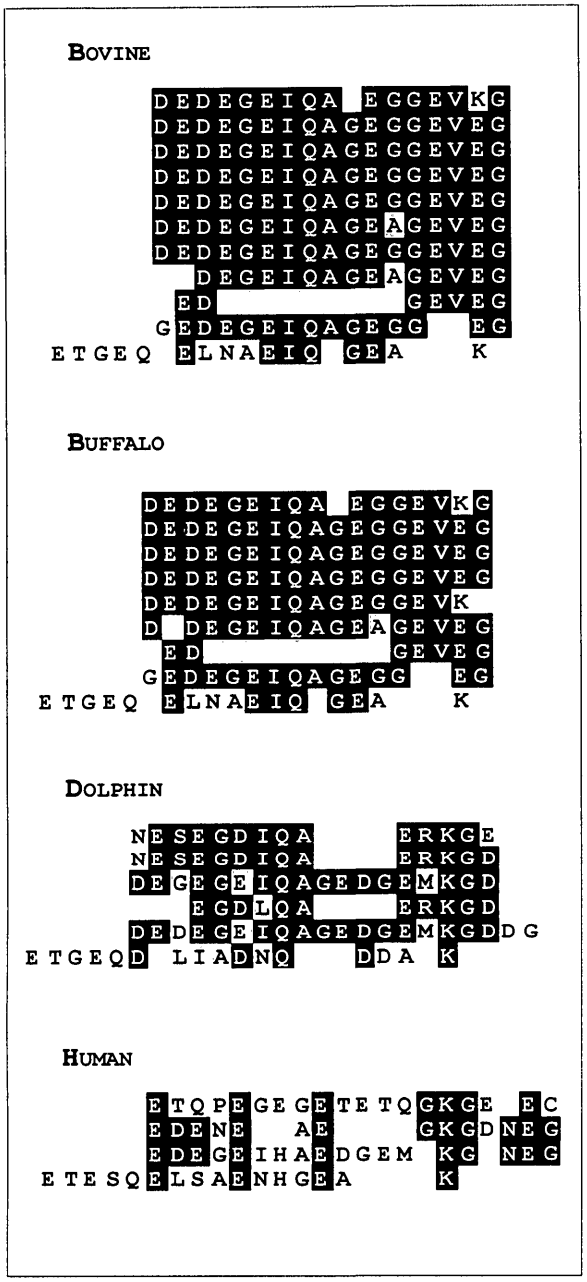

FIGURE 3. Alignment of the repeats consisting of mostly acidic amino acid residues and observed most extensively in the bovine and buffalo sequences.

two repeats were deleted (as indicated here by the removal of repeats 6 and 7), and that, in addition, just a few individual amino acids were changed or deleted. Comparing the dolphin sequence with the bovine sequence showed that not a single one of the bovine repeats was observed in its entirety, although the EGE/DIQA motif was observed five times with only one substitution (L replaces I). Finally, no clear repeats were observed in the human sequence and not a single IQA motif was observed.

DISCUSSION

In this study, we present the cloning and sequencing of the cDNA of the human retinal rod Na-Ca+K exchanger. When comparing the human sequence obtained by us with the published sequence of the bovine rod Na-Ca+K exchanger,[6] the most striking observation is of the poor conservation of the two large domains, which are thought not to be imbedded in the membrane, as judged by hydropathy analysis (Figs. 1 and 2). This is in contrast to other sodium-coupled transporters, such as the NCX1 Na-Ca exchanger, the NEH1 Na-H exchanger, or the alpha subunit of the Na-K ATPase, for which greater than 95% identity has been observed at the amino acid level between clones from different mammalian species, both in putative transmembrane sequences or in putative cytosolic domains (the rod Na-Ca+K exchanger is unusual in that it possesses a large extracellular domain). Because a significant component of the low degree of identity was caused by a series of deletions or insertions, we were concerned that this might reflect artificial deletions or insertions in the cDNA clones in the retinal cDNA library. We have now verified the cDNA sequence with the genomic sequence we obtained while examining the genomic organization of the Na-Ca+K exchanger gene, and we confirmed that the cDNA sequence is correct.

Rods and cones in the retina express in most cases genetically related but different genes for outer segment proteins that are involved in phototransduction—that is, rods and cones express distinct gene products for the cGMP-gated channel.[11] We do not think we obtained a cone Na-Ca+K exchanger because retinal rods greatly outnumber cones in most mammalian retinas, including those of humans and cows; hence, transcripts of rod proteins are expected to greatly outnumber transcripts originating from cones. Moreover, all 12 clones obtained and analyzed from the human retinal cDNA library seem to reflect a single cDNA species because overlapping sequences were identical in all cases. Because we used probes for screening that were based on the bovine rod Na-Ca+K exchanger, we consider it unlikely that we picked up human clones only of the cone exchanger and not of the rod exchanger.

Analysis of an Acidic Repeat Region in the Large Cytosolic Loop

A peculiar example of the variability of domains in the rod Na-Ca+K exchanger sequence was obtained by analyzing the sequence of an acidic amino acid repeat motif observed in the bovine sequence and by comparing it with partial sequences from the dolphin and buffalo. Figure 3 illustrates that the acidic repeat sequence observed in the bovine clone is localized to a part of the sequence that is highly variable across species. Significant changes were already observed when comparing close relatives, such as the bovine and buffalo sequences, whereas most of the repeat sequences disappeared when we compared the bovine to the dolphin sequence (cetaceans are close relatives, of hoofed animals), although some repeats of part of the IQA motif can still be observed. The human Na-Ca+K sequence did not show much evidence for any repeats and does not contain a single IQA motif.

A Revised Sequence for the Bovine Rod Na-Ca+K Exchanger

When we analyzed PCR fragments of the repeat area from both buffalo and bovine cDNA, it seemed that the difference in size between the bovine and buffalo fragments was larger than predicted from a sequence comparison. We sequenced the bovine repeat area, both from our own cDNA and from that obtained from Dr. Reiländer, and we discovered an additional ninth repeat that was missed in the original study on cloning and sequencing of the bovine retinal rod Na-Ca+K exchanger.[6] The fidelity of the repeats in the bovine se-

quence combined with the lack of conservation of this repeat motif in other mammalian species suggests that the repeats observed in the bovine and buffalo sequences arose recently and have not had time to diverge. Poorly conserved acidic repeat motifs have also been observed in the large beta subunit of the rod cGMP-gated channel, which contains a large acidic domain in the N-terminal part of the sequence localized in the cytosol. The bovine sequence contains at least four repeats of the sequence EEGREKEEEG that are not observed in the human beta subunit of the rod cGMP-gated channel,[12] similar to the deletions of the bovine acidic repeats in the human sequence of the rod Na-Ca+K exchanger. The significance of the acidic stretches in the beta subunit of both the cGMP-gated channel and the Na-Ca+K exchanger remains to be established, and why the repeats are observed in both bovine genes but not in the respective human genes must be clarified. Figure 3 suggests that few conservation constraints exist in this region of the protein sequence, as manifested by the rapid evolutionary divergence.

Acknowledgments

The authors thank J. Nathans for the generous donation of samples of a human retinal cDNA library and P. Robinson for the dolphin retinal cDNA library. The authors thank Helmut Reilander for providing the cDNA of the bovine ROS Na-Ca+K exchanger and J. Lytton for helpful discussions and for carefully reading the manuscript.

References

1. Kaupp UB, Koch K-W. Role of cGMP and Ca^{2+} in vertebrate photoreceptor excitation and adaptation. *Annu Rev Physiol.* 1992;54:153-175.
2. Cervetto L, Lagnado L, Perry RJ, Robinson DW, McNaughton PA. Extrusion of calcium from rod outer segments is driven by both sodium and potassium gradients. *Nature.* 1989;337:740-743.
3. Schnetkamp PPM, Basu DK, Szerencsei RT. Na-Ca exchange in the outer segments of bovine rod photoreceptors requires and transports potassium. *Am J Physiol (Cell Physiol).* 1989;257:C153-C157.
4. Schnetkamp PPM. Na-Ca or Na-Ca-K exchange in the outer segments of vertebrate rod photoreceptors. *Prog Biophys Mol Biol.* 1989;54:1-29.
5. Hilgemann, DW, Philipson, KD, Vassort,G, eds. *Sodium-calcium Exchange.* New York: The New York Academy of Sciences; 1996: 1-593.
6. Reiländer H, Achilles A, Friedel U, et al. Primary structure and functional expression of the Na/Ca,K-exchanger from bovine rod photoreceptors. *EMBO J.* 1992;11:1689-1695.
7. Nicoll DA, Longoni S, Philipson KD. Molecular cloning and functional expression of the cardiac sarcolemmal Na^{+}-Ca^{2+} exchanger. *Science.* 1990;250:562-565.
8. Zhaoping L, Matsuoka S, Hryshko LV, et al. Cloning of the NCX2 isoform of the plasma membrane Na^{+}-Ca^{2+} exchanger. *J Biol Chem.* 1994;269:17434-17439.
9. Nicoll DA, Rahamimoff H, Qui Z, et al. Cloning of a third mammalian Na^{+}-Ca^{2+} exchanger, NCX3. *J Biol Chem.* 1996;271:24914-24921.
10. Reid DM, Friedel U, Molday RS, Cook NJ. Identification of the sodium-calcium exchanger as the major ricin-binding glycoprotein of bovine rod outer segments and its localization to the plasma membrane. *Biochemistry.* 1990;29:1601-1607.
11. Bonigk W, Altenhofen W, Muller F, et al. Rod and cone photoreceptor cells express distinct genes for cGMP-gated channels. *Neuron.* 1993;10:865-877.
12. Colville AC, Molday RS. Primary Structure and Expression of the Human β-Subunit and Related Proteins of the Rod Photoreceptor cGMP-gated channel. *J Biol Chem.* 1996;271:32968-32974.

Identification of Two rds/Peripherin Homologs in the Chick Retina

Jian Weng,[1] Teri Belecky-Adams,[2] Ruben Adler,[2] and Gabriel H. Travis[1]*

Purpose. To identify possible homologs of mammalian rds/peripherin in chick photoreceptors.

Methods. An embryonic day-15 chick retinal library was screened by polymerase chain reaction with degenerate oligonucleotide primers derived from conserved segments of the mammalian *retinal degeneration slow* (*rds*) mRNA. The resultant amplification products were used to isolate cDNAs, containing complete coding regions. These clones were studied by nucleotide sequence, Northern blot, and in situ hybridization analyses.

Results. Two new homologs of rds/peripherin were discovered: crds1 and crds2. The predicted crds1 protein is 78%, and the predicted crds2 protein is 54%, identical to mammalian rds/peripherin. The *crds1* mRNA is an abundant 4.4-kb species present in photoreceptors. The *crds2* mRNA is of similar size but is much rarer. No homologs of rom1 were identified in our screen. Developmentally, the *crds1* mRNAs were first detectable at embryonic day 18.

Conclusions. Crds1 likely represents the chick ortholog of mammalian rds/peripherin, whereas crds2 is a more distant homolog. Both share an elongated C-terminal domain, an unusual feature compared with other members of the rds family. (*Invest Ophthalmol Vis Sci.* 1998;39:440-443)

The *retinal degeneration slow* (*rds*) gene is defined by a semidominant mutation in mice with the homozygote phenotype of outer segment nondevelopment and subsequent degeneration of the photoreceptor cell bodies.[1] Mutations in the human homolog of *rds* (*RDS*)[2] have been implicated in multiple inherited retinal dystrophies, including retinitis pigmentosa.[3] The *rds* gene encodes an integral membrane glycoprotein, rds/peripherin, located in the rims of rod and cone outer segment discs.[4,5] In mammals, rds/peripherin is a covalent homodimer that interacts noncovalently with a homodimer of the related protein, rom1, to form a heterotet-

From the [1]Department of Psychiatry and Program in Neuroscience, University of Texas Southwestern Medical Center, Dallas, Texas, and [2]the Wilmer Eye Institute, Johns Hopkins University School of Medicine, Baltimore, Maryland.

Supported by grants from the National Eye Institute and The Foundation Fighting Blindness.

Submitted for publication August 12, 1997; revised October 28, 1997; accepted November 6, 1997.

Proprietary interest category: N.

Reprint requests: Gabriel H. Travis, University of Texas Southwestern Medical Center, 5323 Harry Hines Boulevard, Dallas, TX 75235-9111.